

A Search for Pulsars in Quiescent Soft X-Ray Transients. I.

M. Burgay,¹ L. Burderi,² A. Possenti,^{3,4} N. D'Amico,^{4,5} R. N. Manchester,⁶ A. G. Lyne,⁷
F. Camilo⁸

¹*Dipartimento di Astronomia, Università di Bologna, via Ranzani 1, 40127 Bologna, Italy*

²*Osservatorio Astronomico di Roma-Monteporzio, via Frascati 33, 00127 Monte Porzio
Catone, Italy*

³*Osservatorio Astronomico di Bologna, via Ranzani 1, 40127 Bologna, Italy*

⁴*Osservatorio Astronomico di Cagliari, Loc. Poggio dei Pini, Strada 54, 09012 Capoterra
(CA), Italy*

⁵*Dipartimento di Fisica, Università di Cagliari, Complesso Universitario di Monserrato,
S.P. Monserrato-Sestu Km 0.700, I-09042 Monserrato (CA), Italy*

⁶*Australia Telescope National Facility, CSIRO, P.O. Box 76, Epping, NSW 1710, Australia*

⁷*University of Manchester, Jodrell Bank Observatory, Macclesfield SK11 9DL, UK*

⁸*Columbia Astrophysics Laboratory, Columbia University, 550 West 120th Street, New
York, NY 10027, USA*

ABSTRACT

We have carried out a deep search at 1.4 GHz for radio pulsed emission from six soft X-ray transient sources observed during their X-ray quiescent phase. The commonly accepted model for the formation of the millisecond radio pulsars predicts the presence of a rapidly rotating, weakly magnetized neutron star in the core of these systems. The sudden drop in accretion rate associated with the end of an X-ray outburst causes the Alfvén surface to move outside the light cylinder, allowing the pulsar emission process to operate. No pulsed signal was detected from the sources in our sample. We discuss several mechanisms that could hamper the detection and suggest that free-free absorption from material ejected from the system by the pulsar radiation pressure could explain our null result.

Subject headings: Star: neutron star – millisecond pulsar. Binary star: SXTs

1. Introduction

According to the current paradigm, millisecond pulsars (MSPs) are old neutron stars (NSs) *recycled* through accretion of matter and angular momentum from a mass-losing companion in a binary system (Alpar et al. 1982). Because the accretion process powers a copious X-ray emission, the progenitors of the millisecond pulsars are believed to form a subset of the population of the bright X-ray binaries (see e.g. Bhattacharya & Srinivasan 1995); namely, those classified as Neutron Star Low Mass X-ray Binaries (NS-LMXBs: see e.g. White, Nagase & Parmar 1995 for a review), in which a relatively light K or M star orbits a neutron star and overflows its Roche lobe with the mass transfer is mediated by a keplerian disk.

In a handful of these systems the spin frequency of the NS has been estimated from either coherent pulsations detected during type-I bursts or, indirectly, from the difference of the frequencies of the peaks of the kilohertz quasi periodic oscillations (kHz-QPOs) seen in the X-ray power spectrum of the source (e.g. van der Klis 2000 or Strohmayer 2001). In the latter case, the frequency difference $\Delta\nu$ is interpreted as representative of the spin rate of the NS or of an overtone (Miller, Lamb & Psaltis 1998, but see Stella & Vietri 1998 for a different interpretation). A more accurate analysis has demonstrated that, at least in some cases, $\Delta\nu$ is not constant (e.g. van der Klis et al. 1997; Mendez & van der Klis 1999); however, when both the kHz-QPOs and the coherent pulsations during type-I bursts can be observed, the inferred rotational periods are almost identical and cluster in the interval 1.8–3.8 ms for all the known sources. In the last few years, three transient sources (SAX J1808.4–3658, Wijnands & van der Klis 1998, 1751-305, Markwardt et al. 2002 and XTE 929-314, Galloway et al. 2002) have been discovered to emit coherent pulsations during the entire outburst event. These sources are the first examples of accretion-powered MSPs.

The spin rates inferred from all these sources can be coupled with other requirements imposed by the accretion process for constraining the NS magnetic moment (White & Zhang 1997; Burderi & King 1998; Psaltis & Chakrabarty 1999; Burderi et al. 2002), resulting in values spanning the interval $10^{25} - 10^{27}$ G cm³. In summary, all the available data strongly support the hypothesis that the NS-LMXBs host neutron stars spun up to millisecond periods and having surface magnetic field intensity in the range of those observed in the (spin-powered) MSPs.

Despite all these clues, there is no direct proof of their being the MSP progenitors. Detection of radio signals pulsating at the rotational rate of the NS from some of these sources would provide this proof. A common requirement of the models of the radio emission mechanism from a rotating, magnetized NS is that a radio pulsar phase begins once the space surrounding the NS is free of external matter up to the light cylinder radius r_{lc} (at which

the speed of material rigidly rotating with the NS would be equal to the speed of light):

$$r_{lc} = 4.8 \times 10^6 P_{-3} \text{ cm} \quad (1)$$

where P_{-3} is the pulse period in ms. During the Roche-lobe overflow phase, the plasma spilling through the inner Lagrangian point of the binary system settles into an accretion disc, whose inner rim is located at the so-called magnetospheric radius r_m . That radius results equal to a fraction $\phi \lesssim 1$ of the Alfvén radius, at which the pressure of the (assumed dipolar) NS magnetic field balances the ram pressure of the (assumed spherically) infalling matter:

$$r_m = 1.0 \times 10^6 \phi \mu_{26}^{4/7} \dot{m}_E^{-2/7} m_1^{-1/7} R_6^{-2/7} \text{ cm} \quad (2)$$

Here μ_{26} is the magnetic moment in units of 10^{26} G cm³, \dot{m}_E is the accretion rate in Eddington units (for a 10^6 cm stellar radius the Eddington accretion rate is $1.5 \times 10^{-8} M_\odot \text{ yr}^{-1}$ and scales with the radius of the compact object), m_1 is the NS mass in solar masses, and R_6 is the NS radius R in units of 10^6 cm. All these units are scaled to the parameters of a typical NS–LMXB, as inferred from the aforementioned observations and modeling. As long as r_m is smaller than r_{lc} , the infalling plasma penetrates deeply in the NS magnetosphere and prevents the coherent emission of radio waves. Hence, bright NS–LMXBs showing steady X-ray luminosity are unsuitable targets for observing radio pulses.

However, among the NS–LMXBs known in the Galaxy, $\sim 1/7$ experience recurrent X-ray activity separated by longer phases of relative *quiescence* (Tanaka & Shibazaki 1996). They are known as Neutron Star Soft X-ray Transients (NS–SXTs), belonging to the larger class of the X-ray novae. The physical mechanism driving the transient behaviour of these objects is not fully understood yet (Tanaka & Shibazaki 1996), although a promising model invokes thermal disc instabilities coupled with the stabilizing effects of the illumination of the outer disc by the X-ray from the central source (King, Kolb & Burderi 1996; van Paradijs 1996).

During an outburst, the typical luminosity in the 0.5–10 keV band peaks between 10^{36} and 10^{39} erg/s (Chen, Shrader & Livio 1997) and the frequent observation of type-I bursts unambiguously indicate that massive accretion onto the NS surface is responsible. As a consequence, coherent radio emission cannot occur in this phase. More recently, also the 0.5–10 keV luminosity in quiescence has been detected, at levels ranging between $10^{31.5}$ and 10^{34} erg/s (Campana et al. 1998, Wijnands et al. 2001, Wijnands et al. 2002). Accretion of matter at a lower rate (van Paradijs et al. 1987; Yi et al. 1996) and shock emission from an enshrouded rapidly spinning pulsar (Stella et al. 1994) were originally proposed to account for this lower-luminosity emission. Detailed studies of the X-ray spectrum in quiescence (Rutledge et al. 2001) and of the thermal relaxation of the NS crust during this phase (Colpi et al. 2001) now suggest that the cooling of the periodically warmed up NS surface (Brown

et al. 1998) is the more viable explanation for the bulk of the soft X-ray luminosity in quiescence. If this is the correct interpretation, during the X-ray quiescent phase $\dot{m}_E \sim 0$ and thus, plausibly

$$r_m > r_{lc} . \quad (3)$$

The time scale for the expansion of the magnetospheric radius beyond the light cylinder radius, in response to a sudden drop of the mass transfer rate, is much shorter (Burderi et al. 2001) than the typical duration (\sim years) of a phase of quiescence in a NS–SXT, in principle allowing the radio pulsar to switch on. While inverse Compton scattering from the thermal photons of the quiescent X-ray emission could in principle play a role in absorbing the electrons of the primary beam (hence inhibiting radio emission) in the case of high magnetic field pulsars (Zhang, Qiao & Han 1997, Harding & Muslimov 2002), the same picture seems hardly applicable to the magnetosphere of millisecond pulsars (Supper & Trumper 2000).

With this picture in mind, we have undertaken a systematic deep search for millisecond pulsations at 1.4 GHz in six NS–SXTs during their phases of quiescence. Three of them had not been observed before, while we have significantly increased the sensitivity limits for the three sources (1455–314, 1908+005 and 1745–203) which had been already investigated with negative results (Kulkarni et al. 1992, Biggs & Lyne 1996). The observations and the method of analysis of the data are presented in §2, the results are reported in §3 and are discussed in §4. In §3.1 we discuss the limits introduced in our search by the orbital Doppler effect. The results of a fully accelerated search, which would further improve our limits, will be presented in paper II.

A pulsar binary system has been recently discovered (PSR J1740–5340, D’Amico et al. 2001a) in which the Roche-lobe overflow stage is apparently not yet ended (Ferraro et al. 2001). The MSP is already active and sweeps away the infalling matter preventing accretion onto its surface. This could be the first example of a binary in the *radio-ejection* phase (Burderi, D’Antona & Burgay 2002), believed to be common in many NS–SXTs when the transition from outburst to quiescence occurs (Burderi et al. 2001). Remarkably, the signal from PSR J1740–5340 is eclipsed for about 40% of the time at 1.4 GHz and often strongly disturbed at all orbit phases (D’Amico et al. 2001b), suggesting a bias against the detection of this kind of radio source. Thus, in §4.3 we speculate on the possible absorption of the radiopulsar signal from a NS–SXT when it travels through the plasma that the mass donor companion pours in the binary system also during the X-ray quiescent phase.

2. Observations and data analysis

In Table 1 we present our sample of NS–SXTs, listing the principal observational characteristics derived from X-ray and/or optical data.

Radio observations were made using the Parkes 64-m radio telescope with the central beam of the multibeam receiver at a central radio frequency of 1.4 GHz (cf. Manchester et al. 2001) on 1998 August 2 – 12. The nominal gain and system temperature of the system were 0.67 K/Jy and 22 K, respectively. After detection, the two orthogonally polarized signals are fed through a multichannel filterbank, in order to minimize the pulse broadening due to dispersion in the interstellar medium (ISM). The outputs from each channel are summed in polarisation pairs, integrated and 1-bit digitized every 0.125 ms. The resulting time series are stored on digital linear tapes for offline analysis. In general we used one of two filterbanks: the first splits the signal into 96 3 MHz–wide channels covering a total bandwidth of 288 MHz; the second has 256 channels, each 0.25 MHz wide, for a total bandwidth of 64 MHz. For the source KS 1731–260 (observed in March 2001) we used a filterbank with 512 0.5 MHz channels, giving a total band of 256 MHz, which became available recently.

The observations lasted 1 – 6 hrs for each target; we have split the collected data in segments of different length, typically containing from 2^{22} to 2^{24} samples, corresponding to ~ 9 min and 35 min, respectively. Each segment has been analyzed with `vlsa` (*Very Long Spectral Analysis*, see <http://tucanae.bo.astro.it/pulsar/vlsa/>). In a first stage the data are de-dispersed according to 325 trial DM values ranging from 0.14 to 207.5 pc cm $^{-3}$ for the 96-channel filterbank, or 865 trial DM values in the interval between 0.56 and 2277.2 pc cm $^{-3}$ for the 256-channel filterbank, or 1731 trial values ranging from 0.16 to 1293.6 pc cm $^{-3}$ for the 512-channel filterbank. Lower and upper limits for the searched DMs correspond respectively to a broadening of 0.125 ms (i.e. equal to the sampling time) over the whole band and to a broadening of 2 ms in a single channel (above which the detection of a typical MSP becomes questionable).

Subsequently, each de-dispersed time series is transformed using a Fast Fourier Transform and the highest peaks in the power spectrum (and in the power spectra resulting from 5 steps of harmonic summing; see Manchester et al. 2001) are searched. In summary, for each investigated DM, we have selected periods ranging from 0.5 ms to 200 ms and with a spectral signal-to-noise ratio (S/N) greater than 7.0, storing a list of 640 candidates.

These lists are then sorted in order of decreasing S/N, rejecting, when possible, signals due to known interference. Finally, the time-domain data are folded in 128 subintegrations, using the period of each selected suspect, and the resulting subintegration arrays are searched

for pulsed emission around the nominal period and dispersion measure. The parameters for final pulse profiles having S/N above a given threshold ($\gtrsim 7.0$) are displayed for visual inspection.

3. Results

No radio pulsation with period in the range $0.5 \div 200$ ms has been found in the six Soft X-ray Transients observed. In the following we present the flux density limits of our search. Moreover, we compare them with previous results, when available.

The equation that describes the minimum detectable flux density for a pulsar of period P is (e.g. Manchester et al. 1996):

$$S_{min} = \epsilon n_{\sigma} \frac{T_{sys} + T_{sky}}{G \sqrt{N_p \Delta t \Delta \nu_{MHz}}} \sqrt{\frac{W_e}{P - W_e}} \quad \text{mJy} \quad (4)$$

where n_{σ} is the minimum S/N that we consider (in this case 7.0), T_{sys} and T_{sky} the system noise temperature and the sky temperature in K respectively, G the gain of the radio telescope (in K/Jy), Δt the integration time in seconds, N_p the number of polarizations and $\Delta \nu_{MHz}$ the bandwidth in MHz. ϵ is a factor ~ 1.4 accounting for sensitivity reduction due to digitization and other losses. W_e is the effective width of the pulse:

$$W_e = \sqrt{W^2 + \delta t^2 + \delta t_{DM}^2 + \delta t_{scatt}^2} \quad (5)$$

Its value depends on the intrinsic pulse width W , on the time resolution δt of the receiver and on the broadening of the pulse introduced both by the dispersion of the signal in each channel (δt_{DM}) and by the scattering induced by inhomogeneities in the ISM (δt_{scatt}).

In Figure 1 we show the flux density limits as a function of pulse period for the segments containing 2^{24} samples, for all our targets but SAX J1808.4–3658, for which the period is known. The solid lines refer to the 96×3 MHz filterbank, the dash-dotted lines refer to the 256×0.25 MHz filterbank. For KS 1731–260 the curves refer to the 512×0.5 MHz filterbank. Going towards short periods, the attained sensitivity depends strongly on the adopted DM value. So the lines related to each filterbank split below ~ 100 ms, representing the flux density limits for the nominal DM (i.e. the one inferred from the distance of the source and the ISM electron distribution model by Taylor & Cordes, 1993) and the upper DM value explored in the search, respectively.

For Cen X–4, Aql X–1 and 1745–203 we compare in Fig. 1 our results with those of Kulkarni et al. (1992) and of Biggs & Lyne (1996). We have drawn with dotted lines their

flux density limits, extrapolated at 1.4 GHz using the S_{min} reported by the authors and assuming a typical spectral index 1.7 for the millisecond pulsars. The range of DMs is the same used for plotting our results. We note that our sensitivity limits are significantly better (from 3 to 10 times, depending also on the period) than any previous result.

For those sources for which the pulse period is well known (SAX J1808.4–3658) or for which an indication of the pulse period exists (Aql X–1 and 1731–260), we also plotted (see Figure 2) the flux density limit as a function of the DM, at constant P . The vertical dashed line indicates the nominal DM.

The upper limits on the flux density (for nominal DM and using either the known pulse period or a standard value $P = 3$ ms) are listed in the second column of Table 2 for 35 min long integrations.

Given various uncertainties on the parameters of our apparatus which enter eqs. 4 and 5, we estimate a residual systematic uncertainty of $\sim 25\%$ in the absolute values of the flux densities reported in Table 2 (Camilo et al. 2000).

3.1. Effects of the orbital motion

Because a full acceleration code was not available when the observations were analysed, we now discuss the effects of the orbital motion.

For a binary pulsar, the time of arrival of the pulses (and in turn the observed pulse phase) is affected by the orbital motion. This results in a broadening of the integrated pulse profile and hence in a sensitivity loss during a blind periodicity search. In this case, the effective pulse width can be written as:

$$W_{e_bin} = \sqrt{W_e^2 + \delta t_{bin}^2} \quad . \quad (6)$$

The extra term δt_{bin} accounts for the pulse broadening introduced by the Doppler effect due to the orbital motion:

$$\delta t_{bin} = \frac{1}{8c} a \Delta t^2 \quad (7)$$

where c is the speed of light and a is the line-of-sight component of the acceleration of the NS, supposed constant during the integration time Δt . As δt_{bin} approaches the pulse period P , the pulsating signal is smeared, preventing the discovery of MSPs in strongly accelerated binary systems (cf. Johnston & Kulkarni 1991; Camilo et al. 2000; Jouteux et al. 2002).

For an assigned value of a , δt_{bin} can be significantly decreased only reducing Δt . All the NSs in our sample belong to binary systems: thus, in addition to the standard segments

containing 2^{24} samples, we analysed also shorter time series of 2^{22} samples (corresponding to ~ 9 min), implying a reduction of δt_{bin} of at least a factor 16. In Figure 3 we show the sensitivity loss due to the orbital motion for the case of an integration time of ~ 9 min. The solid line represents the sensitivity to an isolated pulsar, while long-dashed, short-dashed and dotted lines are for a pulsar in a binary system, subjected to a constant acceleration of 5, 15 and 30 m s^{-2} respectively. These values of a span the range of the instantaneous accelerations along the line-of-sight that are experienced by the known millisecond pulsars detected in binary systems.

However, each pulsar undergoes a change of the sign of the line-of-sight acceleration twice a orbit, namely at orbital phases 0.00 and 0.50, when it is in quadrature with the companion star. If a segment of the observation brackets one of these phases and the integration time Δt is a small fraction of the orbital period, the Doppler effect does not significantly affect the detectability of the pulsar in that segment of data. Whenever the total observing time covers at least half a orbit of a binary system, a good segment can always be selected.

According to these considerations, we have listed in Table 2, the minimum pulse period that our search could have detected for the NS–SXTs whose orbital period is known. In particular, we have assumed that the minimum detectable period corresponds to $\delta t_{bin} = 2W_e$, which is $\sim 0.3P$ for a duty cycle of 15%. The value in the fourth column refers to the most favorable situation in which, during a ~ 9 min observation, the NS experiences the minimum line-of-sight acceleration along its (assumed circular) orbit (i.e. when the NS centripetal acceleration is almost perpendicular to the line of sight). The probability that one of the segments in which we have split the observations just coincides with this favorable condition is listed in the fifth column. The value in the last column refers to the worst case, in which the NS apparent motion is almost perpendicular to the line of sight.

For SAX J1808.4–3658, for which we know both the (short) orbital period and the pulse period, and for which our observations covered twice the entire orbit, we analysed segments containing only 2^{21} samples corresponding to 4.4 min. With this choice we are sure that there are at least four segments of the observation where the maximum acceleration along the line-of-sight is $\lesssim 3 \text{ m s}^{-2}$ implying a negligible broadening of the pulse $\lesssim 0.1$ ms.

From Table 2 we see that, with a modest penalty in term of limiting flux density (about a factor 2), our search had a good probability of detecting a millisecond pulsar signal in these binary systems, at least where an indication of the orbital period is available.

It is worth noting that the pulse periods in the sixth column are absolute upper limits: since a significant fraction of the orbit has been always covered by our observations, the line-of-sight acceleration in the best of our segments is certainly less than the maximum possible

acceleration. Moreover, if a millisecond pulsar is bright enough, its signal can appear in a portion of the subintegration array of the folded data even if it is badly smeared by the binary motion over the whole observation. Such a feature would certainly have been recognised.

4. Why a null result ?

Although a full acceleration analysis might improve our detection limit, we have reached sensitivities significantly better than any similar previous search on these six targets, yet we have no detections. We see three possible explanations for this within the framework of the recycling model. These are examined in turn.

4.1. No coherent radio emission in quiescence

A first interpretation is that the simple model presented in §1 fails to predict when the radio emission mechanism switches on in a fast-rotating magnetized neutron star. In particular the condition of equation (3) could be necessary but not sufficient: maybe the conditions for establishment of coherent radio emission require a time longer than the typical time between two accretion phases. On this hypothesis, the class of the NS–SXTs displaying the longest times of quiescence should be preferentially selected for the search of radio pulses.

Another possibility is that the mechanism of accretion contributes to the X-ray luminosity also during quiescence. In this case, the condition (3) is fulfilled if

$$\frac{\dot{m}_{quiesc}}{\dot{m}_{outb}} = \left[\frac{r_m(outb)}{r_m(quiesc)} \right]^{7/2} \lesssim \left[\frac{r_m(outb)}{r_{lc}} \right]^{7/2} \quad (8)$$

where \dot{m}_{quiesc} , \dot{m}_{outb} , $r_m(quiesc)$ and $r_m(outb)$ are the mass transfer rates toward the NS and the magnetospheric radii during the quiescence and during an X-ray outburst. When an approximate value of the spin rate of the NS is available, the rightmost term in equation (8) can be estimated. On the contrary, the leftmost term in equation (8) is usually difficult to estimate because the efficiency η of conversion of the accretion flow into observed X-ray luminosity depends on the regime at which the bulk of the accretion energy is released (Campana et al. 1998). Actually, accretion directly onto the surface of a spinning, magnetized NS is centrifugally inhibited once the magnetospheric radius is outside the corotation radius r_{co} , at which the Keplerian angular frequency of the orbiting matter equals the NS angular speed:

$$r_{co} = 1.5 \times 10^6 P_{-3}^{2/3} m_1^{1/3} \text{ cm.} \quad (9)$$

The light cylinder is always outside the corotation radius, their ratio being $r_{lc}/r_{co} = 3.2 P_{-3}^{1/3} m_1^{-1/3} > 1$ for reasonable values of the parameters. When a NS settles in the so-called *propeller* stage (i.e. $r_{co} < r_m < r_{lc}$), η depends on uncertain factors (Illarionov & Sunyaev 1975) and hence the observed reduction in the X-ray luminosity during the decline from an outburst cannot unequivocally lead to the conclusion that equation (3) is satisfied. Similar caveats hold if the inner part of the accretion disk is bloated, allowing some of the matter to overcome the centrifugal barrier, accreting onto the NS polar caps.

4.2. Geometry and luminosity biases

Even if a radio pulsar is active, its signal could be too weak for being detected at the distance of the Earth and/or the radio beams could miss our line-of-sight. In this section we try to quantify the probability that such geometrical and luminosity factors prevent the detection of radio pulsations at 1.4 GHz from all our six targeted sources.

The average value $f(\rho)$ of the fraction of the sky swept by two conal radio beams of half-width ρ is

$$f(\rho) = \int_0^{\pi/2} f(\rho, \alpha) \sin \alpha d\alpha = (1 - \cos \rho) - (\rho - \frac{\pi}{2}) \sin \rho \quad (10)$$

where α is the angle (supposed randomly distributed) between the magnetic axis (aligned with the radio beams) and the rotational axis and $f(\rho, \alpha) = \cos[\max(0, \alpha - \rho)] - \cos[\min(0, \alpha + \rho)]$ (Emmering & Chevalier 1989).

As a population, the MSPs display wider beams than the longer-period pulsars, but the measured opening angles do not follow the same $P^{-1/2}$ scaling law of the normal pulsars (Kramer et al. 1998). On the contrary, they are spread over a large range of angles for similar values of P . Conservatively assuming the average value $\langle \rho \rangle = 25^\circ$ derived from profile widths measured at 10% intensity by Kramer et al. (1998), we get $f(\rho) = 0.57$. Hence, the probability that the radio beams of all the six targeted sources are missing our line-of-sight is 0.006.

Because of poor statistics and observational biases, the luminosity function of MSPs is difficult to assess. Therefore, in Figure 4 we have plotted the distribution (binned in logarithmic units) of the *pseudo-luminosity* $S_{1400} \times d^2$ for 58 MSPs detected in the Galactic disk and in globular clusters, where S_{1400} is the measured flux density in mJy at 1400 MHz and d is the distance of the source, generally inferred from the dispersion measure, given a model for the distribution of the interstellar ionized matter (Taylor & Cordes 1993). When available, we have used the values of S_{1400} quoted in literature, otherwise we have scaled the

400 MHz flux densities using an average spectral index for the MSPs, $\alpha = 1.7$ (Kramer et al. 1998). Comparing the obtained distribution with our sensitivity limits (indicated in Fig. 4 with an arrow for each observed object) we have roughly estimated for each source the probability that its *pseudo-luminosity* is too faint for detection in our experiment. These probabilities are shown in Fig. 4. Combining these results with the beaming factor, there is a probability of $\sim 20\%$ that the pulsed emission from all the objects in our list would be unobservable at 1.4 GHz. This is not negligible, but can be reduced with deeper searches and/or a larger sample.

4.3. Absorption in the plasma surrounding the binary

It is well known that absorption (see e.g. Thompson et al. 1994 for a review) is a viable mechanism for explaining the absence of observable radio signals from a source surrounded by ionized gas: here we will investigate this hypothesis for the case of a radio pulsar in a NS–SXT.

It has been recently suggested (Burderi et al. 2001) that during their X-ray quiescent phase, most NS–SXTs show the so-called *radio-ejection* phenomenon. During the transition from outburst to quiescence, the mass transfer rate suddenly drops from \dot{m}_{outb} (which determines the X-ray luminosity during the outburst) to a value below \dot{m}_{switch} , at which the condition (3) is satisfied and the NS becomes a source of relativistic particles and magnetodipole emission. The released energy both (*i*) sweeps the environment of the neutron star, allowing coherent radio emission to be switched on (Shvartsman 1970) and (*ii*) expels the gas still leaving the companion star through the inner Lagrangian point of the binary, thus preventing further accretion (Ruderman, Shaham & Tavani 1989).

As pointed out by Burderi et al. (2001), a moderate resurgence of the mass transfer rate \dot{m} to a value just above \dot{m}_{switch} is not sufficient to cause accretion to resume. To quench the radio pulsar, \dot{m} must be restored to at least the outburst value \dot{m}_{outb} . This means that, during the X-ray quiescent phase of a NS–SXT, the mass loss rate from the companion can be quite large (almost equal to the mass transfer rate during the outburst, \dot{m}_{outb}), but nevertheless the matter overflowing the Roche lobe of the companion is swept away by the radiation pressure of the pulsar and leaves the system in the form of a wind.

The possible occurrence of large values of \dot{m} during quiescence suggests that a surrounding wind may be responsible for absorption of the radio emission at any orbital phase. A hydrodynamical simulation of the flow of the plasma from the inner Lagrangian point to the surroundings of the binary is beyond the scope of this paper. Here we are inter-

ested in an order-of-magnitude estimate, to verify that absorption of the radio signal by the ejected plasma can occur for reasonable values of NS–SXT parameters. We adopt the simple hypotheses of free-free absorption in a spherically symmetric outflow (Rasio et al. 1989).

For a system seen edge-on, the minimum electron column density n_e occurs when the NS is in front of the secondary. In this case $n_e = \gamma \int_{R_{L1}}^D N_e dr = \gamma \int_{R_{L1}}^D \rho_{wind}(X + 0.5Y)/m_p dr$, where N_e is the electron density (in cm^{-3}), R_{L1} is the radius of the inner Langrangian point, D is the distance of the system, γ is the fraction of ionized gas, $X \sim 0.7$ and $Y \sim 0.3$ are the hydrogen and helium fractions respectively, and m_p is the proton mass. The density of the swept wind ρ_{wind} is given by the continuity equation $4\pi r^2 \rho_{wind} v_{wind} = \dot{m}$, where v_{wind} is the speed of the wind and \dot{m} the mass loss rate from the secondary. The free-free optical depth can be computed from

$$\tau_{ff} = 0.018 g_{ff} T^{-3/2} \nu^{-2} \int_{R_{L1}}^D N_e^2 dr \quad (11)$$

where ν is the observation frequency, T is the temperature of the gas surrounding the NS and g_{ff} is the Gaunt factor. This term can be written as (Tucker 1975)

$$g_{ff} = \frac{\sqrt{3}}{2\pi} \ln \left[\frac{4}{\xi^{5/2}} \left(\frac{KT}{h\nu} \right) \left(\frac{KT}{Z^2 R_y} \right) \right] \quad (12)$$

where $\xi \sim 1.82$, Z is the atomic number and R_y is the Rydberg constant. Expressing the radius of the inner Lagrangian point in term of the binary parameters $P_{b,h}$ (the orbital period in hours), m_1 and m_2 (the masses of the NS and of the companion) and neglecting the term depending on the inverse of the distance (because $D \gg R_{L1}$), it follows that:

$$\tau_{ff} = 1.63 \times 10^{22} \frac{\dot{m}^2 (X + 0.5Y)^2 \lambda_{21}^2 \ln(\chi T_4^2 \lambda_{21} Z^{-2})}{T_4^{3/2} v_8^2 (m_1 + m_2) P_{b,h}^2 f_{orb}^3} \quad (13)$$

where $\chi = 8.3 \times 10^3$ and $f_{orb} = [1 - 0.462 m_2/(m_1 + m_2)]$. \dot{m} is in units of $M_\odot \text{yr}^{-1}$, v_8 is the velocity of the wind in units of 10^8 km s^{-1} (order of magnitude of the escape velocity from the system), λ_{21} is the wavelength in units of 21 cm and T_4 is the gas temperature in units of 10^4 K . Indeed $T_4 = 1$ is compatible with the kinetic energy of a plasma escaping the binary, but also $T_4 = 10$ could be appropriate, considering that the radiation of the pulsar should heat the surrounding gas. It is useful to write the mass loss from the donor star as a fraction $g \geq 1$ of the mass transfer \dot{m}_{switch} (Burderi et. al 2001)

$$\dot{m} = g \dot{m}_{switch} = 1.3 \times 10^{-12} g \mu_{26}^2 P_{-3}^{-7/3} m_1^{-1/2} . \quad (14)$$

The equations (13) and (14) allow us to compute the value of the parameter g that gives an optical depth $\tau_{ff} > 1$ (thus causing absorption at all orbital phases)

$$g > 6.03 P_{b,h} \frac{T_4^{3/4} v_8 (m_1 + m_2)^{1/2} f_{orb}^{3/2} P_{-3}^{7/3} m_1^{1/2}}{\mu_{26}^2 (X + 0.5Y) \lambda_{21} [\ln(\chi T_4^2 \lambda_{21} Z^{-2})]^{1/2}} . \quad (15)$$

For the NS–SXT to be in quiescence, g must also satisfy

$$g < \dot{m}_{outb}/\dot{m}_{switch} \sim 9.07 \times 10^2 \frac{L_{37}^{outb} R_6 m_1^{3/2}}{\mu_{26}^2 P_{-3}^{-7/3}} . \quad (16)$$

Adopting $\gamma = 1$, $v_8 = 1$, $\lambda_{21} = 1$, $Z = 1$, $T_4 = 1 - 10$, the outburst luminosity $L_{37}^{outb} = 1$ and assuming that the other parameters are those supposed typical of the NS–SXTs ($m_1 = 1.4 M_\odot$, $m_2 = 0.6 M_\odot$, $\mu_{26} = 1$ and $P_{-3} = 3$, implying $\dot{m}_{switch} = 7.2 \times 10^{-14} M_\odot \text{ yr}^{-1}$), there is a large interval of values of g ($10 \lesssim g \lesssim 1000$) which fulfill both the inequalities (15) and (16), provided the orbital period is not too long, $P_{b,h} \lesssim 24$. In summary, complete absorption of the radio signal at 1.4 GHz should be a common phenomenon during the quiescent phase of most NS–SXTs.

In particular, using the available values (see Table 1) of $P_{b,h}$, P_{-3} and L_{37}^{outb} derived from X-ray and/or optical observations (holding the other unknown parameters at the reference values), the inequalities (15) and (16) are satisfied for the sources in our list. Hence, absorption in the gas engulfing the NS–SXTs during quiescence can explain the null result of our search at 1.4 GHz.

In this case, the most favorable moment for detecting a radio pulsar in a SXT would be just at the beginning of the quiescent phase, immediately after the ignition of the radio pulsar emission. At this point, the rate of infall should be a minimum. Later on, during the X-ray quiescent phase, the secondary star would resume a much higher rate of mass loss, not enough for restarting accretion on the NS surface, but enough to completely absorb the radio pulsar signal.

4.3.1. Dispersion smearing

A pulsating signal from a pulsar can become undetectable not only due to absorption, but also if the pulse profile is broadened due to a variation of the dispersion measure during the observation. However, in the following we show that the dispersion smearing alone can hardly explain our results.

Assuming as in §4.3 a fully ionized spherically symmetric isothermal gas leaving the binary, the additional DM_{loc} introduced by the local matter is

$$DM_{loc} = \int_{R_{cav}}^{R_{out}} n_e dr = \int_{R_{cav}}^{R_{out}} \frac{\rho(r)(X + 0.5Y)}{m_p} dr \quad (17)$$

where R_{cav} is the internal radius of the cavity that the pulsar energetic flux creates in the

surrounding gas and R_{out} is the external radius of this cavity, where the density of the gas ρ becomes equal to the ISM density $\rho_{ISM} \sim 2 \times 10^{-24} \text{ g cm}^{-3}$.

Assuming a simple density profile $\rho \propto r^{-2}$ and using the continuity equation for normalizing ρ at its value at R_{out} , from integration of eq (17) it turns out:

$$\text{DM}_{loc} = \frac{\dot{m}(X + 0.5Y)}{4\pi v_{wind} m_p} \left(\frac{1}{R_{cav}} - \frac{1}{R_{out}} \right) = g \, 1.2 \times 10^{18} \frac{\mu_{26}^2 P_3^{-7/3} m_1^{-1/2}}{v_8 a_{l-s}} \text{ cm}^{-2} \quad (18)$$

where a_{l-s} is the orbital separation in light seconds and the other quantities as in §4.3. The right hand of eq (18) has been calculated neglecting the $1/R_{out}$ term, writing $\dot{m} = g \times \dot{m}_{switch}$ (like already done in §4.3) and assuming R_{cav} equal to the orbital separation. Adopting $a_{l-s} = 1$ and using the reference values of §4.3 for the other parameters, we derive

$$\text{DM}_{loc} = g \, 0.025 \quad \text{pc cm}^{-3} \quad (19)$$

On one hand, this estimate ensures that our search has not been limited by additional dispersion due to matter released by the targeted systems: at most one can expect that $g \sim 1000$ (higher values would imply the occurrence of a new phase of accretion which would quench the pulsar radio emission, see previous section), and hence $\text{DM}_{loc} \lesssim 25 \text{ pc cm}^{-3}$, well within the range of our searched values of DM.

On the other hand, eq (15) shows that a true absorption of the signal can be avoided only for $g \lesssim 10 P_{b,h}$, hence for $\text{DM}_{loc} \lesssim 0.25 P_{b,h} \text{ pc cm}^{-3}$. Given the total bandwidth of our observations, the latter inequality corresponds to a dispersive smearing of the pulse $\Delta t_{sm} \lesssim 0.2 P_{b,h} \text{ ms}$ over the entire orbit. The segments of observations that we analysed, anyway, cover only a fraction of the total orbital period, lasting from $\Delta t_{sm}^{seg} \sim 4$ to $\sim 35 \text{ min}$. Hence, the expected smearing produced on every segment is typically of the order:

$$\Delta t_{sm}^{seg} \sim \Delta t_{sm} \frac{\Delta t_{seg,h}}{P_{b,h}} \lesssim 0.3 \Delta t_{seg,h} \lesssim 0.2 \quad \text{ms} \quad (20)$$

where $\Delta t_{seg,h}$ is the segment length in hours. Such values of $\Delta t_{seg,h}$ (in agreement with what we obtain using the *deltaDM* formula from Rasio et al. 1991) are not an obstacle for detecting the pulsating signal. In summary, the dispersion smearing can become a treat for recognizing the pulsating nature of the radio signal from our systems only for values of g for which the signal is already strongly weakened by the free-free absorption. The role of the dispersion smearing could only be enhanced by the presence of strong time-variable clumping and inhomogeneities of the matter at all the orbital phases at which we have observed. In this unlikely case, observations in the continuum would be preferable.

5. Conclusion

We have searched for millisecond pulsations at 1.4 GHz in six neutron-star soft X-ray transient sources during their phases of quiescence. Despite the significant improvement of the sensitivity threshold compared to any similar previous experiment, no pulsed signal was detected.

If coherent radio emission from the rapidly rotating magnetized neutron star occurs in these systems, the probability of having missed it due to its weakness or beaming is only about 25%. Free-free absorption offers a viable alternative interpretation of our null result. We have shown that, during the quiescent phase, the companion to a NS–SXT can lose an amount of gas insufficient to quench the radio emission, but sufficient to completely absorb the radio signal.

N.D’A., A.P. and L.B. are supported by the Ministero della Ricerca Scientifica e Tecnologica (MURST). The Parkes radio telescope is part of the Australia Telescope which is funded by the Commonwealth of Australia for operation as a National Facility

REFERENCES

- Alpar, M. A., Cheng, A. F., Ruderman, M. A. and Shaham, J., 1982, *Nature*, 300, 728
- Bhattacharya, D. & Srinivasan, G. 1995, in: *X-Ray Binaries*, eds. W. H. G. Lewin, J. van Paradijs, E. P. J. van den Heuvel, Cambridge University Press, 495
- Biggs, J. D. & Lyne, A. G. 1996, *MNRAS*, 282, 691.
- Brown, E.F., Bildstein, L., and Rutledge, R.E. 1998, *ApJ*, 504, L95
- Burderi, L., D’Antona, F., and Burgay, M. 2002, *ApJ*, 574, 325
- Burderi, L., Di Salvo, T., Stella, L., Fiore F., Robba, N.R., van der Klis, M., Iaria, R., Mendez, M., Menna, M.T., Campana, S., Gennaro, G., Rebecchi, S, Burgay, M. 2002, *ApJ*, 574, 930
- Burderi, L. & King, A. R. 1998, *ApJ*, 505, L135
- Burderi, L., Possenti, A., D’Antona, F., Di Salvo, T., Burgay, M., Stella, L., Menna, M.T., Iaria, R., Campana, S., D’Amico, N. 2001, *ApJ*, 560, L71
- Camilo, F., Lorimer, D. R., Freire, P., Lyne, A. G., and Manchester, R. N., 2000, *ApJ*, 535, 975
- Campana, S., Colpi, M., Mereghetti, S., Stella, L., and Tavani, M., 1998, *A&A Review*, 8, 279

- Chakrabarty & Morgan, 1998, *Nature*, 394, 346
- Chen, W., Shrader, C. R. and Livio, M. 1997, *ApJ*, 491, 312
- Colpi, M., Geppert, U., Page, D., and Possenti, A. 2001, *ApJ*, 548, L175
- Cordes, J. M. & Lazio T. J. W. 2002, astro-ph/0207156
- D’Amico, N., Lyne, A.G., Manchester, R.N., Possenti, A., and Camilo, F. 2001a, *ApJ*, 561, L89
- D’Amico, N., Possenti, A., Manchester, R.N., Sarkissian, J., Lyne, A.G., and Camilo, F. 2001b, *ApJ*, 561, L89
- Emmering, R. T. & Chevalier, R. A. 1989, *ApJ*, 345, 931
- Ferraro, F.R., Possenti, A., D’Amico, N. and Sabbi, E. 2001, *ApJ*, 561, L93
- Galloway, D. K., Chakrabarty, D., Morgan, E. H., Remillard, R. A. 2002, astro-ph/0206493
- Harding, A. K., Muslimov, A. G. 2002, *ApJ*, 568, 862
- Illarionov, A., & Sunyaev, R. 1975, *A&A*, 39, 185
- Johnston, H. M., & Kulkarni, S. R. 1991, *ApJ*, 368, 504
- Jouteux, S., Ramachandran, R., Stappers, B. W., Jonker, P. G., and van der Klis, M. 2002, *A&A*, 384, 532
- King, A. R., Kolb, U., and Burderi, L. 1996, *ApJ*, 464, L127
- Kramer, M., Xilouris, K. M., Lorimer, D. R., Doroshenko, O., Jessner, A., Wielebinski, R., Wolsczan, A., and Camilo, F. 1998, *ApJ*, 501, 270.
- Kulkarni, S. R., Navarro, J., Vasisht, G., Tanaka, Y., and Nagase, F. 1992, in *X-ray Binaries and Recycled Pulsars*, ed E. P. J. van den Heuvel and S. A. Rappaport, 99, Dordrecht: Kluwer
- Manchester, R. N., Lyne, A. G., Camilo, F., Bell, J. F., Kaspi, V. M., D’Amico, N., McKay, N. P. F., Crawford, F., Stairs, I. H., Possenti, A., Kramer, M., Sheppard, D.C. 2001, *MNRAS*, 328, 17
- Manchester, R. N., Lyne, A. G., D’Amico, N., Bailes, M., Johnston, S., Lorimer, D. R., Harrison, P. A., Nicastro, L. and Bell, J. F, 1996, *MNRAS*, 279, 1235
- Markwardt, C. B., Swank, J. H., Strohmayer, T. E., in’t Zand, J. J. M., Marshall, F. E. 2002, *ApJ*, 575, L21
- Mendez M. & van der Klis, M. 1999, *ApJ*, 517, L21
- Miller, M. C., Lamb, F. K. and Psaltis, D., 1998, *ApJ*, 508, 791

- Ortolani, S., Barbuy, B., & Bica, E. 1994, *A&AS*, 108, 653
- Psaltis, D., Chakrabarty, D., 1999, *ApJ*, 521, 332
- Rasio, F. A., Shapiro, S. L., and Teukolsky, S. A. 1989, *ApJ*, 342, 934
- Rasio, F. A., Shapiro, S. L., and Teukolsky, S. A. 1991, *A&A* 241, L25
- Ruderman, M., Shaham, J., and Tavani M. 1989, *ApJ*, 336, 507
- Rutledge, R. E., Bildsten, L., Brown, E. F., Pavlov, G. G., and Zavlin, V. E. 2001, *ApJ*, 559, 1054
- Shvartsman, V. F. 1970, *Radiofizika*, 13, 1852
- Stella, L., Campana, S., Colpi, M., Mereghetti, S., and Tavani, M. 1994, *ApJ*, 423, L47
- Stella, L., Vietri, M., 1998, *ApJ*, 492, L59
- Strohmayer, T. E. 2001, *AIP Conf. Procs*, Vol 575, "Astrophysical Sources of Gravitational Radiation for Ground-Based Detectors", ed. J.M. Centrella, Philadelphia (astro-ph/0101160)
- Supper, R., Trumper, J. 2000, *A&A*, 357, 301
- Tanaka, Y., & Shibazaki, N. 1996, *ARA&A*, 34, 607
- Taylor, J., & Cordes, J. M. 1993, *ApJ*, 411, 674
- Thompson, C., Blandford, R. D., Evans, C. R., and Phinney, E. S. 1994, *ApJ*, 422, 304
- Tucker, W., 1975, "Radiation processes in astrophysics", Cambridge, Mass., MIT Press, 320
- van der Klis, M. 2000, *ARA&A*, 38, 717
- van der Klis, M., Wijnands, R.A.D., Horne, and K. Chen, W. 1997, *ApJ*, 481, L97
- van Paradijs, J. 1996, *ApJ*, 464, L139
- van Paradijs, J., Verbunt, F., Shafer, R.A., and Arnaud, K.A. 1987, *A&A*, 182, 47
- Verbunt, F., van Kerkwijk, M. H., in't Zand, J. J. M. and Heise, J., 2000, *A&A*, 359, 960
- White, N. E., Nagase, F., and Parmar, A. N. 1995, in: *X-Ray Binaries*, eds. W. H. G. Lewin, J. van Paradijs, E. P. J. van den Heuvel, Cambridge University Press, 1
- White, N.E., & Zhang, W. 1997, *ApJ*, 490, L87
- Wijnands, R., Kuiper, L., in 't Zand, J., Dotani, T., van der Klis, M., and Heise, J., 2002, *ApJ*, 571, 429

Wijnands, R., Miller, J. M., Markwardt, C., Lewin, W. H. G. and van der Klis, M., 2001, *ApJ*, 560, L159

Wijnands, R. & van der Klis, M. 1998, *ApJ*, 507, L63

Yi, I., Narayan, R., Barret, D. and McClintock, J. E, 1996, *A&A*, 120, C187

Zhang, B., Qiao, G. J., Han, J. L. 1997, *ApJ*, 491, 891

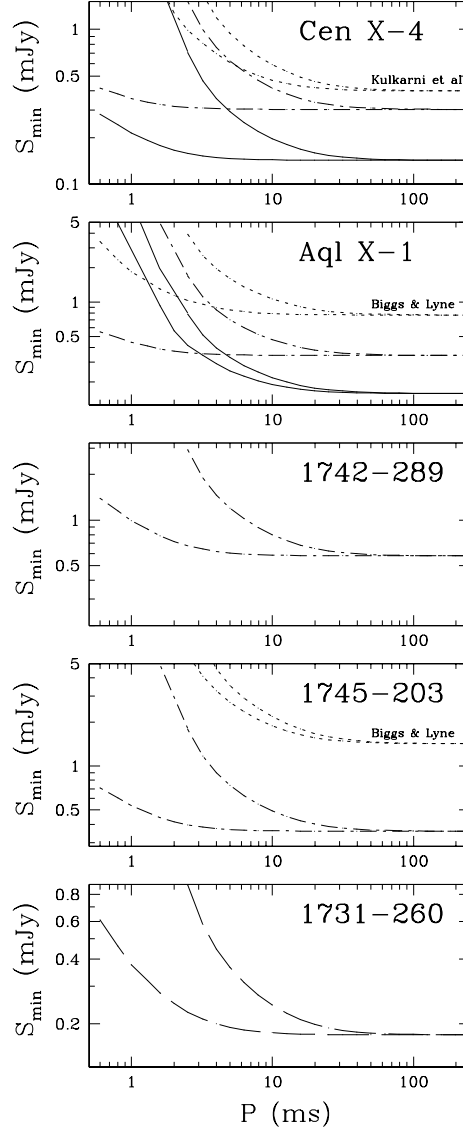


Fig. 1.— Minimum detectable flux density as a function of pulsar period and for two reference values of the DM. For each filterbank, the lower curve refers to the nominal DM and the upper curve to the maximum DM searched (see text). The lines are calculated assuming a duty cycle of 15% and for an integration time ~ 35 min. Solid lines, dotted-dashed lines and dashed lines refer respectively to the 96×3 MHz, to the 256×0.25 MHz and to the 512×0.5 MHz filterbanks. Dotted lines represent the limits obtained by Kulkarni et al. (1992) for Cen X-4 and by Biggs & Lyne (1996) for Aql X-1 and 1745-203.

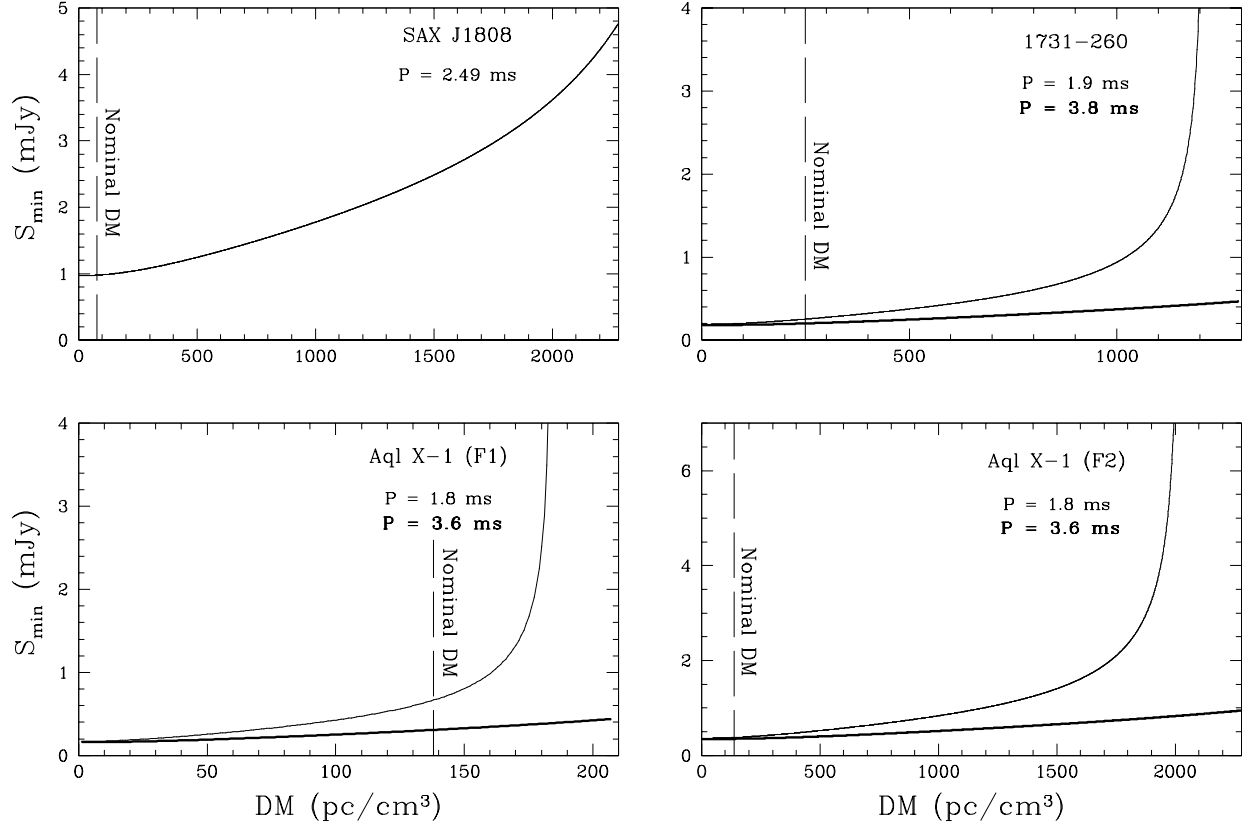


Fig. 2.— Minimum detectable flux density as a function of DM and at constant period for the NS whose pulse period is well assessed or indirectly inferred. For 1731–260 and Aql X–1 we plot the curves for the period detected during Type I burst (thin curve) and for its first subharmonic (thick curve). For Aql X–1 two different plot for two different filterbanks F1 and F2 (respectively the 96×3 MHz filterbank and the 256×0.25 MHz one) are presented.

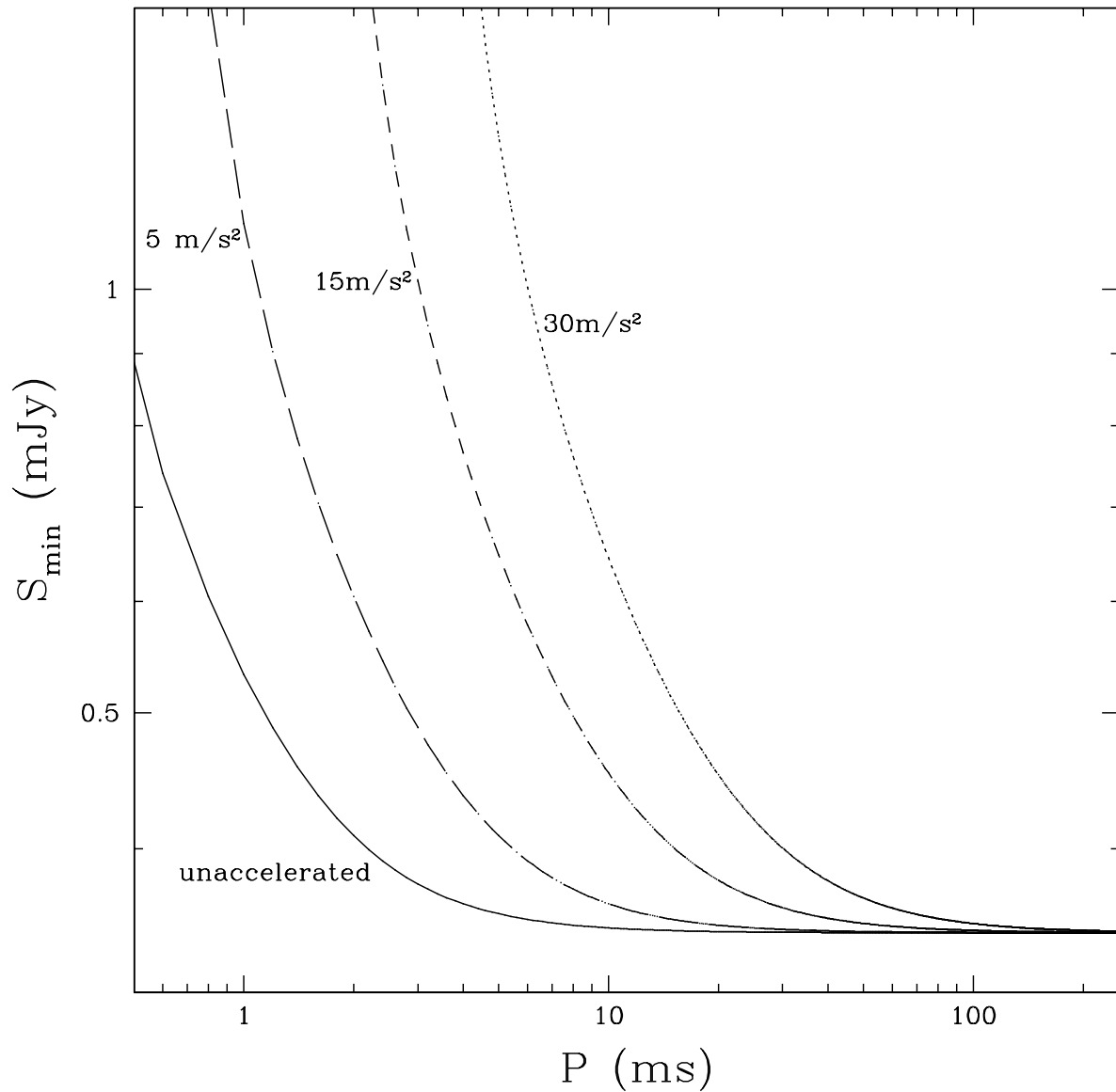


Fig. 3.— Sensitivity of the detection system used for this search as a function of pulse period and acceleration (supposed constant during the integration time). The curves refer to the case of the 96×3 MHz filterbank and of a time series of 2^{22} samples, corresponding to an observation time of ~ 9 min.

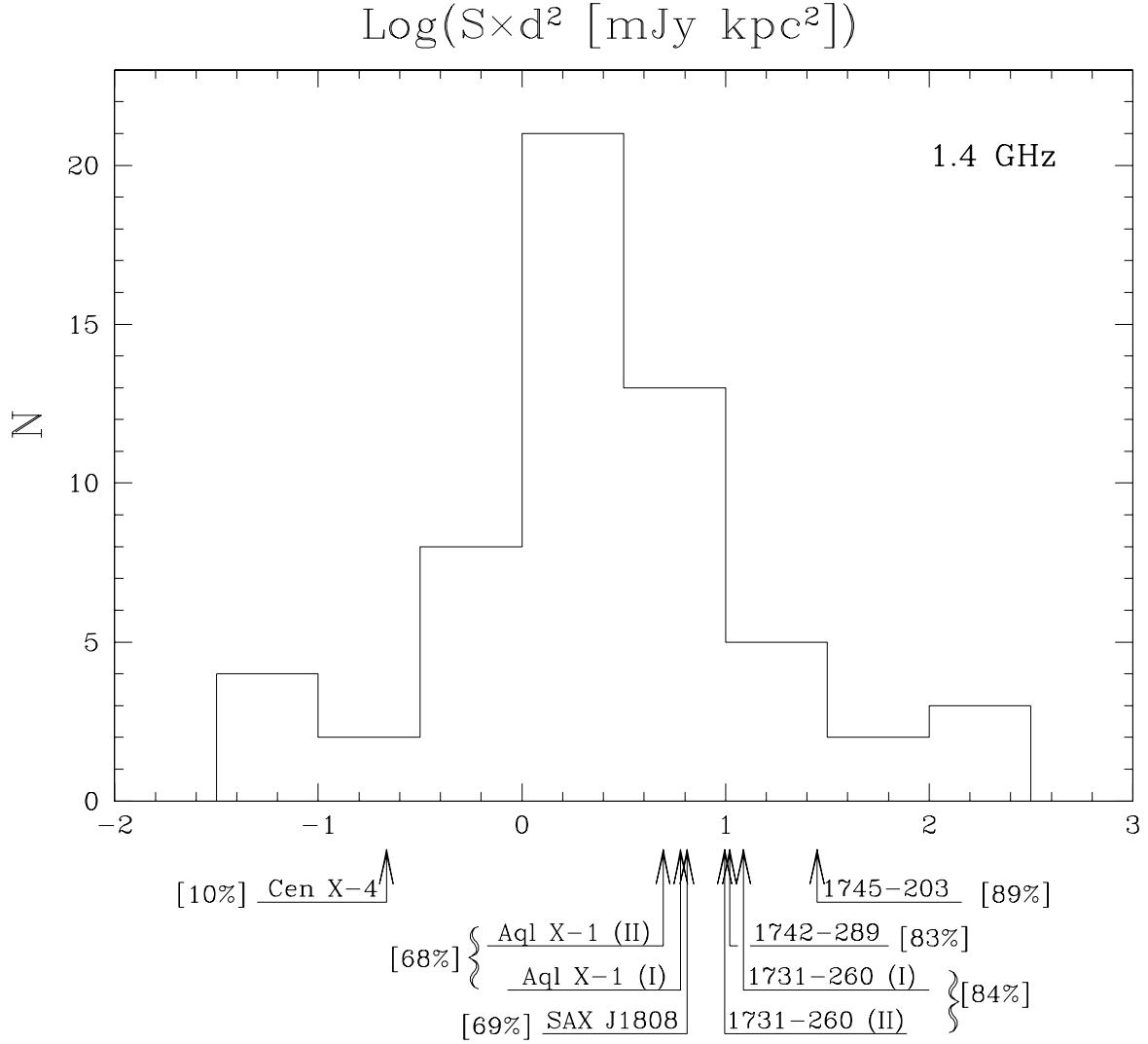


Fig. 4.— Pseudo-luminosity distribution derived from the observation of a sample of 58 MSPs. The arrows indicate the upper limits of the pseudo-luminosity at 1.4 GHz for the SXTs listed in Table 1, derived on the basis of the minimum detectable flux density. For the calculation of S_{min} , we used a 15% duty cycle, the nominal DM and either the known pulse period or a value $P = 3$ ms. For Aql X-1 and 1731-260 we have plotted two different values, one for the period observed during the type I bursts, the other for its first subharmonic. The percentage written near the label of each object represents the probability that the pseudo-luminosity of the source is fainter than the calculated upper limit. These percentages are normalized using the given pseudo-luminosity distribution.

Table 1. Parameters of the sample of Neutron Star Soft X-ray Transients

Source	Other name	Dist (kpc)	Gal l	Coord b	L_X^{outb} (erg/s)	L_X^{quiesc} (erg/s)	DM (pc cm ⁻³)	P_b (h)	P (ms)	Ref.
1455–314	Cen X–4	1.2	332.2	+23.9	4×10^{37}	3×10^{32}	21	15.1	–	[1]
1731–260		7.0	1.1	+3.6	$\sim 10^{37}$	$\sim 10^{33}$	250	–	1.9	[2]
1742–289		4.0	359.9	-0.00	4×10^{38}	$\sim 10^{35}$	238	8.4	–	[1]
1745–203	NGC6440	8.5	7.7	+3.8	3×10^{37}	$\sim 10^{33}$	220	–	–	[3]
1808.4–3658	SAX J1808	2.5	355.7	-7.8	$\sim 10^{36}$	$\sim 10^{32}$	77	2.0	2.5	[4],[5]
1908+005	Aql X–1	~ 4	35.7	-4.1	4×10^{36}	6×10^{32}	138	18.9	1.8	[1],[6]

Note. — For each source we list the most common names, the distance, the Galactic coordinates, the X-ray luminosity during outburst and quiescence, the dispersion measure inferred from the distance and adopting a model for the distribution of the electronic density in the interstellar medium (Taylor & Cordes 1993), the orbital period and the pulse period. The latter is observed in type-I burst for all the sources but SAX J1808.4–3658, which shows coherent pulsations during the entire outburst event.

For 1742–289 the Taylor & Cordes model predicts, for a distance of 8.5 kpc (Ortolani, Barbuy & Bica 1994), a scattering broadening of 7 ms. With this value any millisecond pulsation would be undetectable. However, the outburst luminosity of this source is often greater than the Eddington limit. For those reasons we chose to use a distance $d \sim 4$ kpc, at which the outburst luminosity is comparable to the Eddington limit, giving $\delta t_{scatt} \sim 0.15$ ms and DM ~ 238 pc/cm³. References: [1] Campana et al. 1998; [2] Burderi et al. 2002; [3] Verbunt et al. 2000; [4] Wijnands et al. 2002; [5] Chakrabarty & Morgan 1998; [6] Rutledge et al. 2001.

Table 2. Upper limits on the flux density

Source	S_{min} (35 min) (mJy)	S_{min} (8.75 min) (mJy)	P_{min} (best acc) (ms)	\mathcal{P} (best acc)	P_{min} (worst acc) (ms)
1455–314	0.15	0.31	0.39	62%	6.54
1731–260	0.25	0.51	—	—	—
1742–289	0.64	1.29	0.76	100%	9.15
1745–203	0.39	0.62	—	—	—
1808.4–3658 [†]	—	0.98	0.29	100%	1.28
1908+005	0.38	0.76	0.15	42%	3.07

Note. — For each source it is reported the minimum flux density calculated at the nominal DM and using either the known pulseperiod or a standard value $P = 3$ ms, for observation lasting 35 min (second column) and 8.75 min (third column). For the nominal DM we used the value given by the Taylor & Cordes model (1993). If we use Cordes & Lazio (2001) model for the ISM electron distribution we obtain a higher value of the nominal DM, and hence a slightly higher value of the quoted S_{min} , for all sources but Aql X–1 (for wich the two models give roughly equal DMs). The fourth and the sixth columns take into account the effects of the orbital motion showing the minimum pulse period detectable by our search in the best and in the worst case respectively. The fifth column reports the probability of occurrence of the best case.

[†] For this source the values refer to segments of data 4.4 min long.